The ERBB4/HER4 receptor tyrosine kinase regulates gene expression by functioning as a STAT5A nuclear chaperone

Christopher C. Williams,[1] June G. Allison,[6] Gregory A. Vidal,[2] Matthew E. Burow,[3] Barbara S. Beckman,[4] Luis Marrero,[5] and Frank E. Jones[1]

[1]Department of Biochemistry, [2]Department of Structural and Cellular Biology, [3]Department of Medicine, and [4]Department of Pharmacology, Tulane University Health Sciences Center, Tulane Cancer Center, and [5]Louisiana State University Health Sciences Center, Gene Therapy Program, The Morphology and Imaging Core Laboratory, New Orleans, LA 70112
[6]Northshore High School, Saint Tammany School Board, Slidell, LA 70461

In the lactating breast, ERBB4 localizes to the nuclei of secretory epithelium while regulating activities of the signal transducer and activator of transcription (STAT) 5A transcription factor essential for milk-gene expression. We have identified an intrinsic ERBB4 NLS (residues 676–684) within the ERBB4 intracellular domain (4ICD) that is essential for nuclear accumulation of 4ICD. To determine the functional significance of 4ICD nuclear translocation in a physiologically relevant system, we have demonstrated that cotransfection of ERBB4 and STAT5A in a human breast cancer cell line stimulates β-casein promoter activity. Significantly, nuclear localization of STAT5A and subsequent stimulation of the β-casein promoter requires nuclear translocation of 4ICD. Moreover, 4ICD and STAT5A colocalize within nuclei of heregulin β1 (HRG)-stimulated cells and both proteins bind to the endogenous β-casein promoter in T47D breast cancer cells. Together, our results establish a novel molecular mechanism of transmembrane receptor signal transduction involving nuclear cotranslocation of the receptor intracellular domain and associated transcription factor. Subsequent binding of the two proteins at transcription factor target promoters results in activation of gene expression.

Introduction

The ERBB family of receptor tyrosine kinases, namely the EGF receptor (EGFR), ERBB2/HER2/Neu, ERBB3, and ERBB4, regulate cellular proliferation, differentiation, and programmed cell death in a growth factor–dependent manner. Several recent reports have described nuclear translocation of EGFR, ERBB3, and ERBB4 (Lin et al., 2001; Ni et al., 2001; Lee et al., 2002; Offterdinger et al., 2002). ERBB4 is the only member of the ERBB family that encodes both putative nuclear localization and nuclear export signals providing a mechanism for regulating nuclear accumulation of the ERBB4 protein. In addition, recent reports have detailed a unique proteolytic cleavage mechanism leading to nuclear translocation of the ERBB4 intracellular domain (4ICD). Essential for ERBB4 nuclear translocation is the sequential proteolytic cleavage of ERBB4 at the cell membrane to release 4ICD. These processing events are catalyzed by TNFα-converting enzyme (TACE) and presenilin-dependent γ-secretase activity (Rio et al., 2000; Ni et al., 2001; Lee et al., 2002).

ERBB4 has multiple functions during embryogenesis (Gassmann et al., 1995) and ERBB4 expression has recently been shown to be essential during breast development and lactation (Long et al., 2003; Tidcombe et al., 2003). Critical ERBB4 activities in the breast are mediated, in part, through ERBB4-induced activation of the signal transducer and activator of transcription (STAT) family member, STAT5A. ERBB4-mediated activation of STAT5A in the pregnant and lactating breast results in STAT5A transactivation of milk genes with γ-interferon activation sites (GAS) within their promoters, including β-casein and whey acidic protein (Long et al., 2003). Interestingly, both ERBB4 and STAT5A localize to the nuclei of secretory epithelium during lactation and STAT5A nuclear localization requires ERBB4 expression

C.C. Williams and J.G. Allison contributed equally to this work.

The online version of this article contains supplemental material.

Correspondence to Frank E. Jones: fjones@tulane.edu

Abbreviations used in this paper: 4ICD, ERBB4 intracellular domain; ChIP, chromatin immunoprecipitation; dsRed, *Discosoma* red fluorescent protein; EGFR, EGF receptor; GAS, γ-interferon activation sites; HRG, heregulin β1; LMB, leptomycin B; Prl, prolactin; STAT, signal transducer and activator of transcription; TACE, TNFα-converting enzyme; YAP, yes-associated protein.

The Journal of Cell Biology, Vol. 167, No. 3, November 8, 2004 469–478
http://www.jcb.org/cgi/doi/10.1083/jcb.200403155

(Long et al., 2003). Furthermore, experiments demonstrating coimmunoprecipitation of ERBB4 and STAT5A (Jones et al., 1999) raise the possibility that these two proteins exist in a functionally important nuclear complex.

Despite detailed biochemical descriptions of ERBB4 proteolytic cleavage events and several reports of nuclear ERBB receptors, the molecular mechanisms and physiological relevance of ERBB nuclear translocation remain to be determined. Our previous demonstration of nuclear localization of ERBB4 within mammary secretory epithelium coincident with the essential contribution of ERBB4 to STAT5A regulated milk-gene expression (Long et al., 2003) led us to hypothesize that 4ICD nuclear translocation modulates transactivation of STAT5A target genes. Here, we support our hypothesis through the identification and inactivation of an intrinsic ERBB4 NLS. We further demonstrate that nuclear 4ICD uses a novel signal transduction mechanism to potentiate the expression of STAT5A target genes.

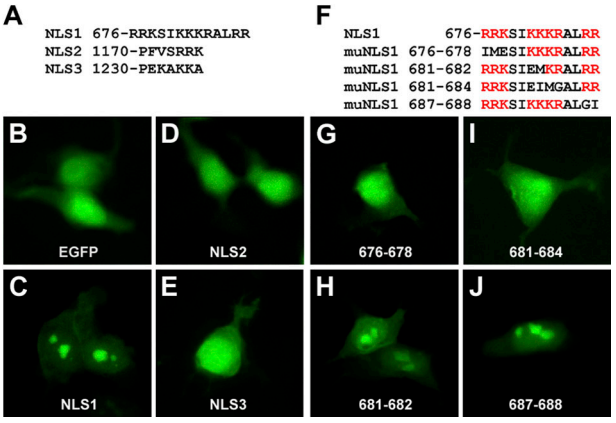

Figure 1. **Identification of a minimal ERBB4 sequence that enhances EGFP nuclear accumulation.** (A) ERBB4 residues representing putative NLSs fused to the amino terminus of EGFP. (B–E) Localization by deconvolution microscopy of indicated NLS-EGFP constructs 48 h after transfection of HEK 293T cells. (F) Basic residues (red) altered in NLS1-EGFP fusions. (G–J) Localization by deconvolution microscopy of indicated NLS1-EGFP mutants 48 h after transfection of HEK 293T cells.

Results

Identification of an ERBB4 basic residue stretch sufficient to enhance nuclear accumulation of EGFP

As an experimental approach toward the identification of an intrinsic ERBB4 NLS, we tested the ability of three independent ERBB4 basic residue stretches positioned within 4ICD (Fig. 1 A; Srinivasan et al., 2000) to enhance nuclear translocation of EGFP. When transiently transfected into HEK 293T cells the EGFP (Fig. 1 B) vector control and amino-terminal EGFP fusions of NLS2 (Fig. 1 D) and NLS3 (Fig. 1 E) displayed identical patterns of diffuse cytoplasmic localization accompanied by basal levels of nuclear accumulation. An NLS1-EGFP fusion (Fig. 1 C) on the other hand exhibited distinct nuclear accumulations within subnuclear structures resembling nucleoli. Although these results do not exclude a role for NLS2 and NLS3 in nuclear translocation, consistent with our results, a putative juxtamembrane EGFR NLS, with basic residue clusters similar to the ERBB4 NLS1, was shown to mediate nuclear translocation of β-galactosidase (Lin et al., 2001).

Having identified a minimal ERBB4 sequence that enhances EGFP nuclear accumulation, we next attempted to identify regions essential for NLS1-mediated EGFP nuclear accumulation by incorporating several independent mutations within the three basic residue clusters of NLS1 (Fig. 1 F; basic residues indicated in red). Nuclear accumulation of muNLS1-EGFP (681–682; Fig. 1 H) and muNLS1-EGFP (687–688; Fig. 1 J) indicates that NLS1 can sustain residue substitutions at these sites. Substitutions at residues 676–678 (Fig. 1 G) or 681–684 (Fig. 1 I), however, returned nuclear accumulation of NLS1 fused to EGFP to basal levels. These results suggest that ERBB4 residues 676–684 constitute a functional NLS.

NLS1 mediates nuclear translocation of the 4ICD

We created NLS1 inactivating base substitutions at residues 681–684 (Fig. 1 F) in two versions of the wild-type ERBB4 protein, one fused at the carboxyl terminus with EGFP (ERBB4muNLS-EGFP) and the other harboring tandem carboxyl-terminal Flag epitope tags (ERBB4muNLS). We confirmed that ERBB4 fused to EGFP retained the ability to associate with and activate STAT5A fused at the amino terminus to *Discosoma* red fluorescent protein (dsRed; Red-STAT5A; Fig. S1, available at http://www.jcb.org/cgi/content/full/jcb.200403155/DC1). Furthermore, we show that altering ERBB4 residues 681–684 does not impact ERBB4 growth factor stimulation or proteolytic processing to release 4ICD (Fig. S2, available at http://www/jcb.org/cgi/content/full/jcb.200403155/DC1).

We next examined the contribution of NLS1 to ERBB4 nuclear translocation by deconvolution microscopy of MCF-7B human breast cancer cells (Burow et al., 2001) transiently transfected with ERBB4-EGFP or ERBB4muNLS-EGFP. In untreated cells, the majority of ERBB4-EGFP was localized to the cellular membrane and perinuclear region (Fig. 2, A–C). Treatment of transfected cells with the ERBB4 ligand heregulin β1 (HRG) dramatically enhanced both perinuclear and nuclear accumulation of ERBB4/4ICD (Fig. 2, G–I and Y). ERBB4 also encodes three putative nuclear export signals harbored within 4ICD (Ni et al., 2001). Therefore, we treated transfected cells with the inhibitor of chromatin region maintenance 1/exportin 1 nuclear export protein, leptomycin B (LMB; Kudo et al., 1999). LMB treatment resulted in nuclear retention of >90% of basal-activated ERBB4/4ICD (Fig. 2, M–O and Y) and >80% of HRG-activated ERBB4/4ICD (Fig. 2, S–V and Y). Strikingly, mutation of NLS1 completely abolished ERBB4/4ICD nuclear translocation under each condition tested (Fig. 2 Y), indicating that NLS1 of ERBB4 is a functionally active intrinsic NLS mediating nuclear translocation of 4ICD. In another experimental system, NIH 3T3 cells were stably transfected to express physiological levels of ERBB4-Flag or ERBB4muNLS-Flag. Despite equivalent levels of HRG-induced tyrosine phosphorylation, nuclear accumulation of

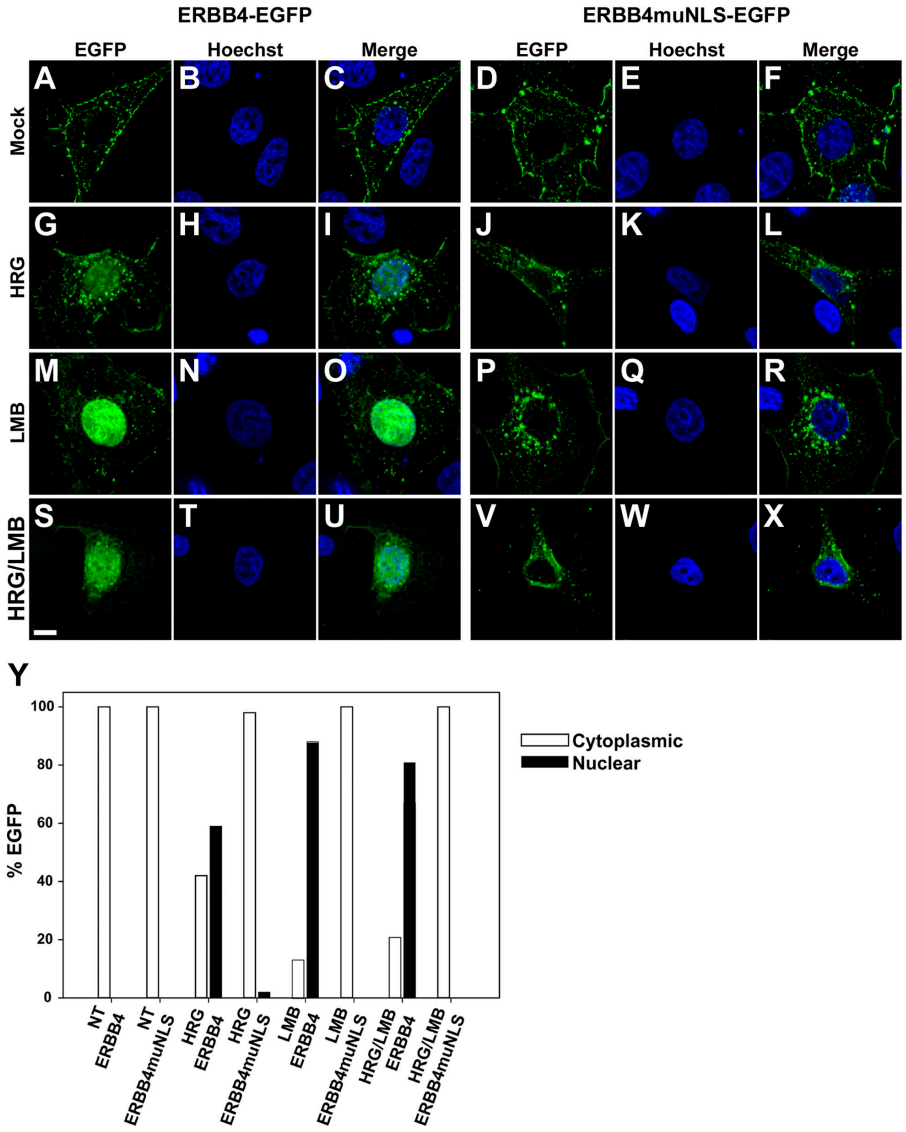

Figure 2. **ERBB4 nuclear translocation requires an intact NLS1.** MCF-7B cells were transfected with ERBB4-EGFP (A–C, G–I, M–O, and S–U) or ERBB4muNLS-EGFP (D–F, J–L, P–R, and V–X) harboring base substitutions (K681E, K682I, K683M, R684G) within NLS1. Immediately before fixation in 4% PFA at 48 h after transfection cells were treated by (A–F) mock stimulation, (G–L) stimulation with 50 ng/ml of HRG for 30 min at RT (HRG), (M–R) incubation with 10 ng/ml of LMB for 12 h (LMB), or (S–X) a combination of HRG and LMB treatments (HRG/LMB). After fixation, nuclei were stained with Hoechst dye and observed by deconvolution microscopy. (Y) The mean percentage of EGFP fluorescence in the cytoplasmic or nuclear compartments for each treatment was determined by analyzing EGFP intensities from 10 transfected cells. Bar, 8 μm.

ERBB4/4ICD was only observed in cells expressing ERBB4-Flag (Fig. S3, available at http://www.jcb.org/cgi/content/full/jcb.200403155/DC1).

The contribution of NLS1 to 4ICD nuclear localization was confirmed by Western blot analysis of nuclear extracts isolated from transiently transfected and HRG-stimulated MCF-7B cells. Despite high levels of ERBB4 and 4ICD protein within the membrane/cytosolic fractions from ERBB4-Flag and ERBB4muNLS-Flag–transfected cells (Fig. 3, lanes 2 and 3), 4ICD was not detected within the nuclei of mock-stimulated cells (Fig. 3, lanes 5 and 6). As predicted, 4ICD was detected in nuclear extracts from HRG-stimulated ERBB4-Flag transfected cells (Fig. 3, lane 11), however, HRG failed to drive nuclear translocation of 4ICD in ERBB4muNLS–transfected cells (Fig. 3, lane 12). Some membrane ERBB4 contamination was observed in nuclear extracts of HRG-treated cells (Fig. 3, lanes 11 and 12). Together, our cellular microscopy and biochemical data strongly implicate NLS1 as a functional ERBB4 NLS mediating nuclear translocation of 4ICD.

ERBB4 nuclear translocation regulates STAT5A transactivation

We next determined the function of nuclear 4ICD using a physiologically relevant experimental system. Our recent in vivo data indicates that ERBB4 activation of STAT5A in the mammary gland regulates lactational expression of the essential milk-genes β-*casein* and *whey acidic protein* (Jones et al., 2003; Long et al., 2003). As an extension of these observations we next determined if ERBB4 stimulates STAT5A transactivation of a bovine β-casein promoter positioned upstream of the luciferase reporter gene.

Relative to the empty vector control, independent expression of STAT5A or ERBB4 resulted in insignificant levels of β-casein promoter activity (Fig. 4). Coexpression of ERBB4 and STAT5A, however, resulted in a >40-fold increase in β-casein reporter activity (Fig. 4) demonstrating for the first time that an ERBB receptor directly regulates STAT5A transactivation. As predicted activation of the β-casein promoter was abolished when STAT5A was cotransfected with an ERBB4 mutant lacking intrinsic kinase activity (ERBB4KD; Sartor et al., 2001) or

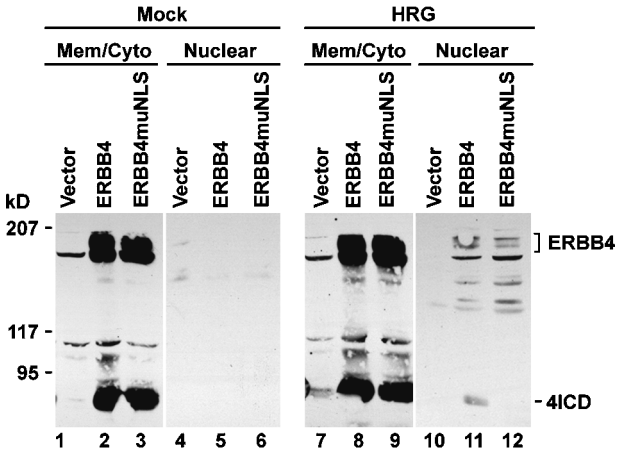

Figure 3. **Nuclear accumulation of the 4ICD requires an intact NLS1.** Transfected MCF-7B cells were mock stimulated or treated with 50 ng/ml of HRG for 30 min. Cell lysates were prepared and separated into membrane/cytosolic (Mem/Cyto) and nuclear fractions. The lysates were analyzed by PAGE and Western blot using an antibody directed against the carboxyl-terminal Flag epitope tags of ERBB4 and ERBB4muNLS. The 80-kD ERBB4 cleavage product, 4ICD, was detected in Mem/Cyto fractions of ERBB4 (lanes 2 and 8) and ERBB4muNLS (lanes 3 and 9) transfected cells but only in the nuclear fractions of HRG-stimulated ERBB4 transfected cells (lane 11). A high molecular mass nonspecific band was detected in Mem/Cyto extracts prepared from vector control transfected cells (lanes 1 and 7) and nuclear extracts prepared from HRG-stimulated ERBB4 and ERBB4muNLS transfected cells (lanes 11 and 12). Each experiment detected a variable but low level of full-length ERBB4 contamination in nuclear extracts prepared from HRG-stimulated cells (lanes 11 and 12).

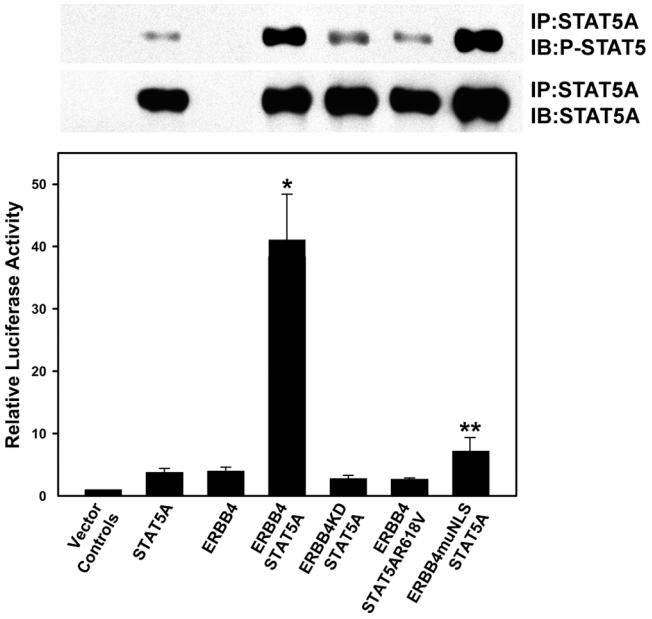

Figure 4. **ERBB4 nuclear translocation modulates STAT5A stimulation of the β-casein promoter.** MCF-7B cells were cotransfected with the bovine β-casein promoter fused to luciferase and plasmids expressing the indicated cDNAs. Cell lysates were prepared at 2 d after transfection and luciferase activity was determined using standard methods. Results are reported as fold increase in luciferase activity relative to β-casein promoter luciferase cotransfected with empty vector controls. ERBB4/STAT5A stimulation of the β-casein promoter was significantly greater than each of the other treatments (* indicates $P < 0.05$). ERBB4muNLS/STAT5A stimulation of the β-casein promoter was significantly greater than the ERBB4 kinase-dead (ERBB4KD/STAT5A) and STAT5A SH2 domain mutant (ERBB4-Flag/STAT5AR618V) negative controls (** indicates $P < 0.05$). Each treatment was preformed in duplicate and the entire experiment was repeated three times. STAT5A was immunoprecipitated from lysates prepared for luciferase assay and analyzed by Western blot for STAT5A expression and activation by phosphorylation at the regulatory Y694 (top).

when ERBB4 was cotransfected with a STAT5A protein harboring a mutation that ablates SH2 activity (STAT5AR618V) and thus disrupting the interaction between ERBB4 and STAT5A (Fig. 4; Jones et al., 1999). Strikingly, when STAT5A was cotransfected with ERBB4 harboring an inactive NLS1 (ERBB4muNLS), a significant and dramatic decrease in STAT5A transactivation was observed (Fig. 4). This ablation of STAT5A transactivation was observed despite equivalent levels of ERBB4 and ERBB4muNLS-induced STAT5A phosphorylation at the regulatory STAT5A Y694 (Fig. 4, top). Together, these results clearly indicate that nuclear translocation of 4ICD regulates STAT5A transactivation of the β-casein milk-gene promoter, implicating a physiologically important role for 4ICD nuclear translocation during milk-gene expression.

Mutation of the ERBB4 NLS prevents STAT5A nuclear accumulation

In the mouse, both ERBB4 and activated STAT5A localize to the nuclei of mammary secretory epithelium while providing essential functions during lactation (Long et al., 2003; Tidcombe et al., 2003). Interestingly, STAT5A fails to encode essential basic residues constituting a STAT NLS originally identified in STAT1 (Melen et al., 2001; Meyer et al., 2002). Therefore, we examined the possibility that ERBB4 regulates STAT5A transactivation by augmenting STAT5A nuclear translocation. We cotransfected MCF-7B cells with ERBB4-EGFP and Red-STAT5A, determined the subcellular localization of each protein by deconvolution microscopy, and quantitated the levels of ERBB4-EGFP and Red-STAT5A colocalization using a pixel correlation algorithm.

Deconvolution microscopy revealed ERBB4 accumulation at the cell membrane of mock-treated cells with a high level of cytoplasmic STAT5A colocalization, probably representing STAT5A associated with constitutively activated ERBB4 protein (Fig. 5 A, top, and Fig. 5 B). When cotransfected cells were stimulated with HRG, pronounced nuclear accumulation and dramatic nuclear colocalization of 4ICD and STAT5A was observed (Fig. 5 A, bottom, and Fig. 5 B). The punctate pattern of 4ICD/STAT5A nuclear colocalization resembles sub-nuclear structures referred to as nuclear speckles. The exact function of nuclear speckles remains controversial but appear to be sites of splicing machinery assembly associated with highly active transcription (Lamond and Spector, 2003).

Although significant levels of cytoplasmic and perinuclear ERBB4/4ICD and STAT5A colocalization was observed in cells cotransfected with STAT5A and ERBB4-muNLS (Fig. 5 C, top, and Fig. 5 D), both proteins were excluded from the nucleus, even under conditions of HRG stimulation (Fig. 5 C, bottom, and Fig. 5 D). Together, these results imply that nuclear translocation and subsequent nuclear colocalization of 4ICD and STAT5A requires an intact ERBB4 NLS, implicating 4ICD as a nuclear chaperone for STAT5A.

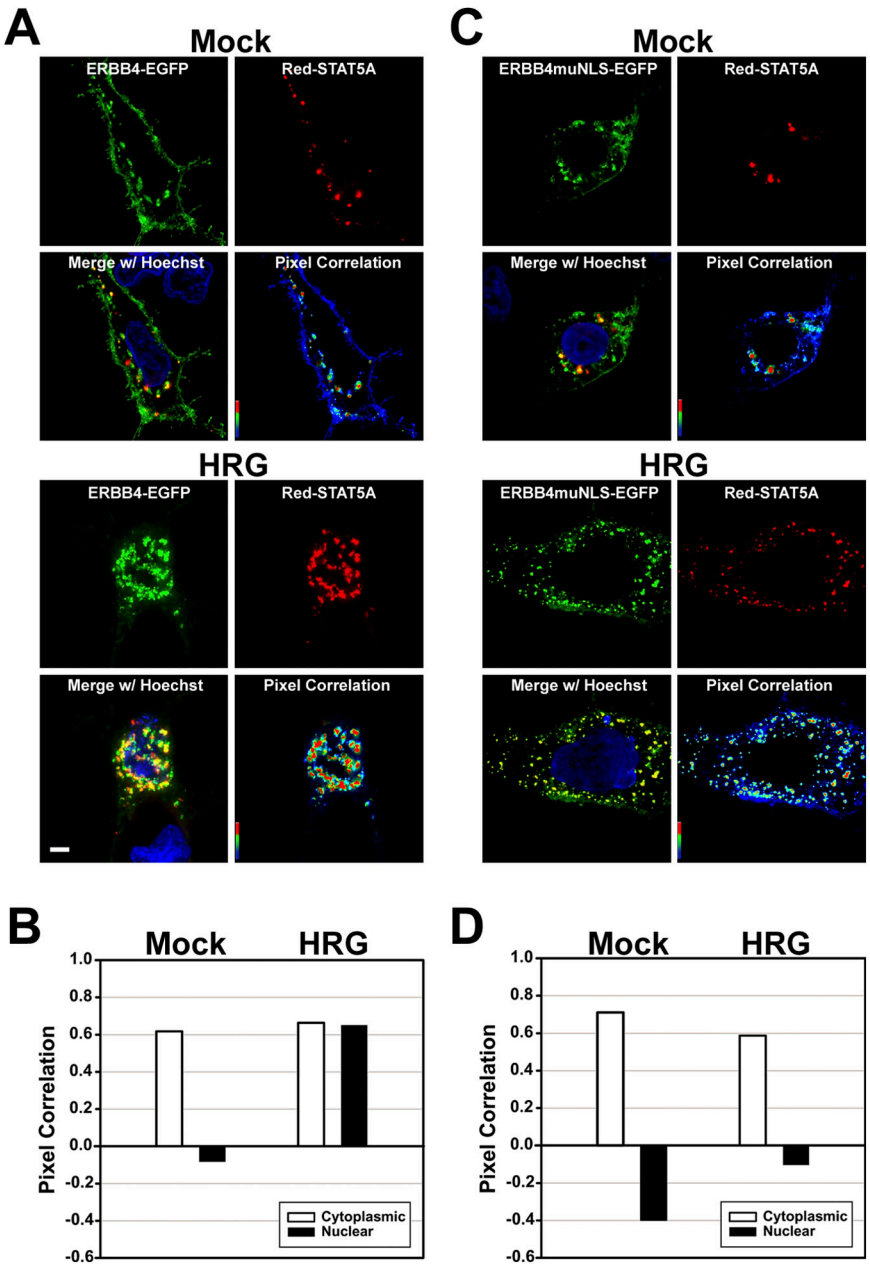

Figure 5. **Activated ERBB4 mediates nuclear translocation of coexpressed STAT5A.** MCF-7B cells were cotransfected with (A and B) Red-STAT5A and ERBB4-EGFP or (C and D) Red-STAT5A and ERBB4muNLS-EGFP. Immediately before fixation in 4% PFA at 48 h after transfection, cells were mock stimulated (Mock) or stimulated with 50 ng/ml of HRG for 30 min at RT (HRG). After fixation, cells were stained with Hoechst dye and observed by deconvolution microscopy. Cytoplasmic and nuclear colocalization of ERBB4 (green) and STAT5A (red) of 10 cotransfected cells in the merged image (Merge w/Hoechst) was measured using a pixel correlation algorithm (B and D). Bar, 5 μm.

ERBB4/4ICD associates with STAT5A in the cytosol and at the β-casein promoter

Perinuclear colocalization of ERBB4/4ICD and STAT5A (Fig. 5) suggests that the two proteins exist in a cytosolic complex before nuclear translocation. We have reported previously an interaction between the ERBB4 holoreceptor and STAT5A (Jones et al., 1999). To determine if 4ICD also interacts with STAT5A we cotransfected COS-7 cells with ERBB4-Flag or ERBB4muNLS-Flag and STAT5A and probed STAT5A immunoprecipitates for ERBB4/4ICD using a Flag antibody. Consistent with our previous results, the ERBB4 holoreceptor was detected in STAT5A immunoprecipitates from lysates of cells transfected with ERBB4-Flag/STAT5A and ERBB4muNLS-Flag/STAT5A (Fig. 6 A, lanes 5, 6, 11, and 12). Significantly, 4ICD was detected in the same samples indicating that STAT5A and 4ICD exist in a cytosolic complex. An interaction between cytosolic 4ICD and STAT5A supports the contention that perinuclear 4ICD chaperones associated STAT5A across the nuclear membrane. Due to the high levels of ERBB4 constitutive activation in transient transfected cells (Fig. S2) HRG treatment had little impact on the association between ERBB4/4ICD and STAT5A.

Nuclear colocalization of 4ICD and STAT5A raised the possibility that the two proteins exist in a functionally important complex bound to the promoters of STAT5A target genes. To determine if 4ICD and STAT5A associate at STAT5A target promoters in vivo we performed a chromatin immunoprecipitation (ChIP) assay in T47D breast cancer cells and examined HRG-stimulated association of 4ICD and STAT5A at distal and proximal regions of the endogenous β-*casein* promoter (Fig. 6 B). In mock-stimulated T47D cells antibodies against ERBB4 and STAT5A precipitated a small but detect-

able amount of the proximal (−294/−1) and distal (−4719/−4276) β-casein promoter regions (Fig. 6 C, lanes 3 and 4), harboring a single and three STAT5A binding GAS sites, respectively (Fig. 6 B; Winklehner-Jennewein et al., 1998). As predicted, stimulation of T47D cells with prolactin (Prl) resulted in increased STAT5A but not 4ICD binding to the β-casein promoter (Fig. 6 C, lanes 7 and 8). Significantly, a dramatic increase in both STAT5A and 4ICD binding to the β-casein promoter was observed after HRG stimulation of T47D cells (Fig. 6 C, lanes 11 and 12). As predicted, Prl and HRG failed to stimulate binding of STAT5A or 4ICD to a region of the β-casein promoter lacking GAS sites (−923/−590). Together, our results imply that 4ICD modulates STAT5A transactivation by first functioning as a STAT5A nuclear chaperone, then 4ICD may function as a transcriptional cofactor at STAT5A target promoters. Indeed, we (unpublished data) and others (Ni et al., 2001) have observed transactivation activity harbored within 4ICD.

Discussion

We have identified a novel signal transduction pathway in which the ERBB4 transmembrane receptor regulates gene expression by functioning as a nuclear chaperone for the STAT5A transcription factor. After nuclear cotranslocation of the 4ICD and STAT5A both proteins associated in a complex at the β-*casein* promoter. Based on our observations, we propose a unique mechanism for ERBB4 regulation of STAT5A-stimulated gene activation (Fig. 7). Recent evidence indicates that HRG stimulation and subsequent proteolytic processing of ERBB4 at the cell surface results in release of 4ICD from the cell membrane (Rio et al., 2000; Ni et al., 2001; Lee et al., 2002). Here, we propose that 4ICD first accumulates in the perinuclear region. Then in a process requiring an intact NLS (residues 676–684) a 4ICD perinuclear/nuclear equilibrium is established. An efficient nuclear export mechanism, which is inhibited by LMB, maintains the equilibrium toward perinuclear 4ICD. When coexpressed, activated ERBB4 associates with the STAT5A transcription factor in a STAT5A SH2-dependent manner (Jones et al., 1999). STAT5A remains associated with 4ICD and the two proteins colocalize in the perinuclear region. Nuclear translocation and subsequent nuclear colocalization of both proteins requires an intact ERBB4 NLS. Interestingly, we also observe pronounced nuclear retention of 4ICD when coexpressed with STAT5A, indicating that STAT5A impairs 4ICD nuclear export, thereby dramatically shifting the 4ICD perinuclear/nuclear equilibrium in favor of nuclear accumulation. Finally, activation of the ERBB4/STAT5A signal transduction pathway and subsequent nuclear cotranslocation of 4ICD and STAT5A results in binding of the two proteins at STAT5A target gene promoters culminating in a robust stimulation of STAT5A target genes possibly potentiated by transactivation activity harbored within 4ICD. Together, our results suggest a novel molecular mechanism to explain our in vivo observations demonstrating ERBB4/STAT5A cooperative activation of essential milk-genes during lactation (Jones et al., 2003; Long et al., 2003).

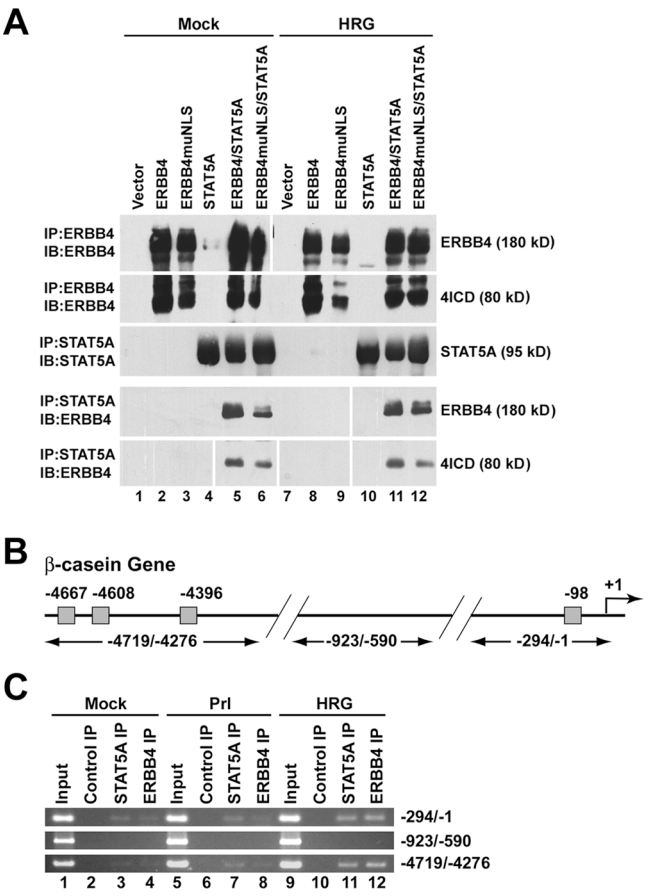

Figure 6. **The 4ICD and STAT5A associate in vivo and bind to the endogenous β-*casein* promoter.** (A) 4ICD is associated with STAT5A. COS-7 cells were transfected with the indicated expression plasmids and at 2 d after transfection cells were mock stimulated or stimulated with 50 ng/ml of HRG for 30 min at RT. ERBB4 and STAT5A immunoprecipitates were prepared from cell lysates, resolved by PAGE, and probed for ERBB4 and/or STAT5A by Western blot. White lines indicate that intervening lanes have been spliced out. (B) Schematic of β-*casein* gene indicating positions of primers for semi-quantitative PCR of distal (−4719/−4276) and proximal (−294/−1) upstream regulatory regions and a promoter region lacking STAT5A GAS binding sites (−923/−590). Gray boxes indicate positions of STAT5A GAS binding sites (Winklehner-Jennewein et al., 1998). (C) Semi-quantitative PCR amplification of DNA bound to ERBB4 and STAT5A isolated by ChIP assay. T47D breast cancer cells were mock stimulated, stimulated with 5 μg/ml of ovine Prl, or stimulated with 50 ng/ml of HRG for 30 min at RT. PFA cross-linked chromatin was immunoprecipitated using control rabbit IgG or antibodies directed against ERBB4 and STAT5A and subjected to 35 cycles of PCR. Input chromatin was prepared from cross-linked and cleared cell lysates using standard DNA precipitation procedures and amplified by PCR as above. PCR amplified samples were resolved on a 2% agarose gel and stained with ethidium bromide.

Of the four ERBB family members nuclear localization of three receptors, namely EGFR (Lin et al., 2001), ERBB3 (Offterdinger et al., 2002), and ERBB4 (Ni et al., 2001), has been described recently. The lack of a confirmed ERBB NLS, however, has hampered progress toward identification of the functional implications of ERBB nuclear translocation. Nevertheless, ligand activation of EGFR results in association of nuclear EGFR with the cyclin D1 promoter and EGF stimulation of the cyclin D1 promoter fused to luciferase requires EGFR expression. Interestingly, EGFR harbors independent transacti-

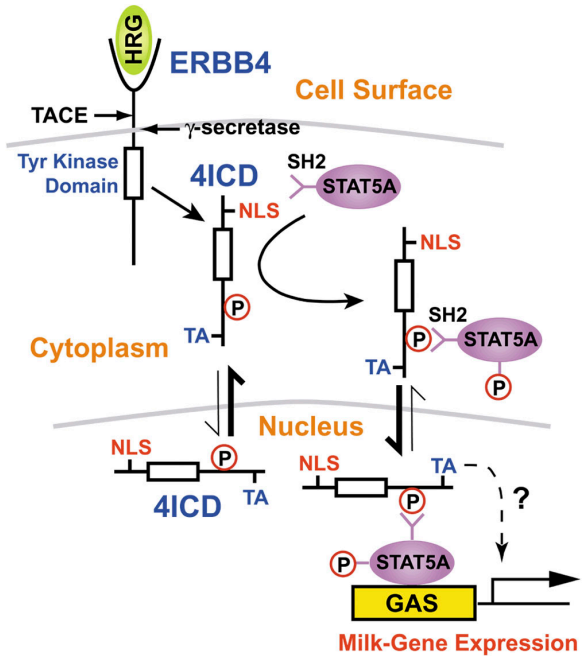

Figure 7. **A model for ERBB4 regulation of STAT5A-stimulated gene expression.** Growth factor–stimulated ERBB4 undergoes sequential proteolytic processing at the cell membrane by TACE and presenilin-dependent γ-secretase to release 4ICD. 4ICD accumulates in the perinuclear region where a perinuclear/nuclear equilibrium is established favoring perinuclear over nuclear 4ICD. Cytosolic STAT5A associates with activated ERBB4/4ICD in an SH2 domain–dependent manner and STAT5A is phosphorylated at multiple residues including the regulatory Y694 (Jones et al., 1999, 2003). Nuclear cotranslocation of 4ICD and STAT5A requires an intact ERBB4 NLS. The two nuclear proteins bind to STAT5A target promoters containing GAS thereby stimulating expression of STAT5A regulated milk-genes including β-casein and whey acidic protein (Long et al., 2003). STAT5A mediates nuclear retention of 4ICD resulting in a dramatic shift from perinuclear and nuclear accumulation of 4ICD. Interestingly, 4ICD harbors transactivation activity (TA) which may directly augment STAT5A target gene expression.

vation activity raising the possibility of direct gene activation by nuclear EGFR (Lin et al., 2001). Similarly, we (unpublished data) and others (Ni et al., 2003) have identified transactivation activity harbored within 4ICD. Association of 4ICD with STAT5A at STAT5A target promoters may potentiate STAT5A stimulation of gene expression. Our identification of a functional ERBB4 NLS may also be relevant for EGFR nuclear translocation. The ERBB4 NLS and the putative EGFR NLS (Lin et al., 2001) share basic residue stretches positioned immediately downstream of the transmembrane domain. These observations imply that ERBB4 and EGFR nuclear activities are functionally and mechanistically similar.

Nuclear translocation of ERBB4 does however require proteolytic processing at the cell membrane to release the 4ICD nuclear protein, whereas both EGFR and ERBB3, appear to be transported to the nucleus as holoreceptors (Lin et al., 2001; Offterdinger et al., 2002). Inhibitors of presenilin-dependent γ-secretase activity suggest that this ERBB4 processing event is essential for 4ICD nuclear accumulation (Ni et al., 2001; Lee et al., 2002). Interestingly, we have identified a transmembrane valine (V673) residue critical for γ-secretase–mediated ERBB4 cleavage and mutation of this residue (V673I) abolishes 4ICD nuclear translocation (unpublished data). A similarly positioned valine within the Notch1 transmembrane is essential for γ-secretase processing of this receptor and nuclear translocation of the Notch1 intracellular domain (Schroeter et al., 1998). EGFR and ERBB3, on the other hand, encode a leucine (L642) and a phenylalanine (F644), respectively, at the same transmembrane position and therefore lack a canonical γ-secretase cleavage site. This difference in proteolytic processing at the cell membrane may explain why EGFR and ERBB3 are transported to the nucleus as holoreceptors whereas 4ICD is the predominant ERBB4 nuclear protein.

STAT5A-mediated nuclear retention of 4ICD raises two unresolved questions, specifically, what is the mechanism of 4ICD nuclear retention and what, if any, is the physiological consequence of retaining 4ICD in the nucleus. Although the exact mechanism of STAT5A regulated nuclear retention of 4ICD remains unclear, retention of STAT proteins is mediated by an intrinsic DNA binding domain (Herrington et al., 1999; Meyer et al., 2003). STAT5A DNA binding activity may similarly inhibit nuclear export of 4ICD associated with STAT5A at STAT5A target gene promoters. In support of this contention, we observe binding of STAT5A and 4ICD at endogenous β-casein promoter regions harboring STAT5A DNA binding sites. Alternatively, mechanisms regulating ERBB4 nuclear export may be masked or sterically hindered through an association with STAT5A.

Our data clearly indicate that ERBB4 can indirectly regulate gene expression by functioning as a nuclear chaperone for STAT5A. Additionally, association of 4ICD and STAT5A at STAT5A target promoters suggests that 4ICD may function as a transcriptional cofactor. The aforementioned transactivation activity harbored within 4ICD may directly cooperate with STAT5A in the selection and transactivation of target genes. In addition, ERBB4 may indirectly modulate STAT5A transactivation through nuclear translocation of 4ICD associated transcriptional coactivators. For example, the yes-associated protein (YAP) transcription factor and its isoforms and independently expressed 4ICD colocalize within nuclei of cotransfected cells. Furthermore, a direct association between YAP and 4ICD is essential for ERBB4 transactivation activity in a GAL4 assay (Komuro et al., 2003). Together, these observations raise the intriguing possibility of STAT5A DNA-binding localizing 4ICD to specific target genes with subsequent 4ICD modulation of target gene selection or transactivation or both.

Although several transmembrane receptors have been detected in the nucleus, the functional significance of cell surface receptor nuclear translocation remains an intriguing biological problem. Our current results indicate that ERBB4 and STAT5A use a novel cooperative mechanism of gene regulation with 4ICD functioning as a nuclear chaperone for STAT5A and STAT5A mediating nuclear retention of colocalized 4ICD associated at STAT5A target promoters. Both ERBB4 and STAT5A localize to the nuclei of breast epithelium while supplying essential functions during breast development and lactational milk-gene expression (Jones et al., 2003; Long et al., 2003; Tidcombe et al., 2003), providing a physiologically important basis for our current observations. In conclusion, we offer a functional explanation for nuclear transloca-

tion of transmembrane receptors and describe a unique signal transduction paradigm that may have important implications during developmental regulation of gene expression.

Materials and methods

ERBB4 cDNA

The human ERBB4 cDNA used in these experiments has been sequenced in its entirety (Plowman et al., 1993) and represents the JM-a isoform (Elenius et al., 1997). This isoform retains both TACE and γ-secretase recognition sequences and is therefore an ERBB4 isoform that undergoes complete proteolytic processing at the cell surface after ligand stimulation.

Plasmid constructs

The three putative ERBB4 NLS sequences (Srinivasan et al., 2000) and mutations of NLS1 each including a 5′ EcoR1 overhang, Kozak sequence, start ATG, and 3′ BamH1 site were independently fused to the amino terminus of EGFP by ligating EcoRI–BamHI digested pEGFP-N1 (CLONTECH Laboratories, Inc.) with the annealed oligonucleotides described in Table I.

The plasmid pERBB4-EGFP expressing full-length human ERBB4 with a carboxyl-terminal EGFP fusion was constructed in three steps. First, the intermediate construct pcDNA ERBB4 was generated by trimolecular ligation joining EcoRV–NotI digested pcDNA5/TO (Invitrogen), the 3.8-kb SalI (site filled with T4 DNA polymerase)–BamHI fragment from pLXSN-ERBB4 (Riese et al., 1995), and the 315-bp BamHI–NotI digested PCR product generated from pLXSN-ERBB4 using the forward primer upstream of the unique BamHI site 5′-ATGCCAGAGAAGGCCAAG (nt 3705–3723; Plowman et al., 1990) and the reverse primer harboring a unique EcoRV site, tandem Flag epitope tags, and NotI site downstream of an amber stop codon 5′-ATAAGAATGCGGCCGCCTACTTGTCATCGTCGTCCTTGTAGTCCTTGTCATCGTCGTCCTTGTAGTCGATATCCACCACAGTATTCCGGTG (nt 3949–3931; Plowman et al., 1990). Next, the ERBB4 ORF with tandem carboxyl-terminal Flag epitope tags was subcloned into pBluescript SK I (Stratagene) by ligating AflI (site filled with T4 DNA polymerase)–NotI-digested pcDNA-ERBB4 with ClaI (site filled with T4 DNA polymerase)–NotI-digested pBluescript SK I, generating the plasmid pBl-ERBB4. Finally, pERBB4-EGFP was generated by ligating the 4.1-kb fragment lacking Flag epitope tags from SalI–EcoRV digested pBl-ERBB4 with XmaI (site filled with T4 DNA polymerase)–SalI digested pEGFPN3 (CLONTECH Laboratories, Inc.).

The ERBB4 NLS1 was altered in pERBB4-EGFP through residue substitutions at K681E, K682I, K683M, R684G to generate the plasmid pERBB4muNLS-EGFP in multiple steps. The 2.3-kb fragment from SpeI–BclI digested pBl-ERBB4 harboring NLS1 was subcloned into the same sites of pBluescript SK I to generate pBl-ERBB4 S/B. NLS1 was mutagenized in pBl-ERBB4 S/B to generate the clone pBl-ERBB4muNLS by PCR-mediated site-directed mutagenesis using a downstream primer corresponding to the T7 promoter, an upstream primer corresponding to the T3 promoter, and the mutation incorporating oligonucleotide primer pair 5′-AGCATCGAAATGATAAGGGCCTTGAGAAGATTCTTGGAA (nt 2085–2106; Plowman et al., 1990) and 5′-CAAGGCCCTTATCATTTCGATGCTCTTCCTTCTAACATA (nt 2091–2053; Plowman et al., 1990). NLS1 mutagenic primers were designed to generate a novel EcoO109I site. The intermediate plasmid pERBB4muNLS-EGFP-Int was generated by ligating the 2.3-kb SpeI–BclI fragment from pBl-ERBB4muNLS and the 4.5-kb SpeI–BclI fragment from pERBB4-EGFP. The final pERBB4muNLS-EGFP construct was generated by ligating the 1.9-kb SpeI fragment from pERBB4-EGFP into SpeI digested pERBB4muNLS-EGFP-Int.

The constructs pERBB4-Flag and pERBB4muNLS-Flag were generated by replacing the 1.8-kb AclI–NotI fragments from pERBB4-EGFP and pERBB4muNLS-EGFP, respectively, with the corresponding AclI–NotI fragment from pBl-ERBB4.

The construct pRed-STAT5A was generated by tri-molecular ligation of the HindIII–NruI digested PCR product from amplified pEF-STAT5A (Jones et al., 1999) using the upstream primer 5′-ATCCCAAGCTTCCACCATGGCGGGCTGGATT supplying a Kozak start site and unique HindIII site and the primer 5′-ATCTGAAGGTGCTTCTGGGA positioned down stream of the unique NruI site, the ~2.0-kb pEF-STAT5A NruI–EcoRI fragment, and HindIII–EcoRI digested pdsRed1-C1 (CLONTECH Laboratories, Inc.). The construct pRed-STAT5AY694F was generated by replacing the ~2.0-kb NruI–EcoRI fragment from pRed-STAT5A with the same fragment from pEF-STAT5AY694F (Jones et al., 1999). The construct pEF-STAT5AR618V has been described elsewhere (Jones et al., 1999).

Cell lines and transfections

The human embryonic kidney cell line HEK 293T, NIH 3T3, and COS-7 cell lines were obtained from ATCC and cultured in DMEM with 10% FBS and 2 mM L-glutamine. The dramatic growth inhibitory effect of ectopic ERBB4 expression (Sartor et al., 2001) precluded analysis of ERBB4 nuclear localization in many common mammalian cell lines. Therefore, we performed all functional assays in the MCF-7 human breast cancer cell line MCF-7B, which was modified to stably overexpress BCL-2 (Burow et al., 2001). MCF-7B cells were cultured in MEM containing 10% FBS, 1 mM Na-pyruvate, and 2 mM L-glutamine.

Transfections were performed on 2×10^5 cells in 35-mm tissue culture dishes or 0.8×10^5 cells in a two-chamber tissue culture treated glass slide with 1 μg of each transfected DNA using Fugene6 transfection reagent (Roche) as described by the manufacturer. In each experiment transfected cells were harvested at 48 h after transfection.

NIH 3T3 cell lines stably expressing ERBB4-Flag (NIH-H4) or ERBB4muNLS (NIH-H4muNLS) were generated by cotransfecting NIH 3T3 in 35-mm tissue culture dishes at 70% confluence with 0.2 μg of pLXSN and 2 μg of pERBB4-Flag or pERBB4muNLS-Flag using Fugene6 as described above. At 2 d after transfection cells were selected by transferring the contents of a 35-mm dish to a 100-mm tissue culture dish containing selection media (growth media with 2 mg/ml of G418 [Roche]). After 5 d of selection, resistant colonies were pooled and maintained in selection media for an additional 2 wk. Successful stable expression of ERBB4-Flag and ERBB4muNLS-Flag was confirmed by Flag Western blot analysis of cell lysates.

Western blot analysis

Immunoprecipitations from transfected cell lysates or total cell lysates were separated on a 7.5% polyacrylamide gel, transferred to Hybond ECL (Amersham Biosciences) membrane, and analyzed by Western blot as described previously (Jones et al., 1999). Primary antibodies were anti-ERBB4 (Santa Cruz Biotechnology, Inc.), anti-STAT5A (Santa Cruz Biotechnology, Inc.), anti-P-Stat5 (Zymed Laboratories), anti–Flag-M2 (Sigma-Aldrich), and anti–phospho-tyrosine (Santa Cruz Biotechnology, Inc.).

Preparation of membrane and cytosolic cellular fractions

Membrane and cytosolic fractions were isolated from COS-7 cells transfected with vector control, ERBB4-Flag, or ERBB4muNLS-Flag using a modification of a protocol published elsewhere (Lee et al., 2002). In brief, at

Table I. **ERBB4 DNA sequences fused to EGFP**

Construct	Human ERBB4 sequence	ERBB4 residues	Altered residues
EGFPN1	NA	NA	NA
NLS1-EGFP	AGAAGGAAGAGCATCAAAAAGAAAAGAGCCTTGAGAAGA	R676-R688	NA
NLS2-EGFP	CCTTTTGTTTCTCGGAGAAAA	P1170-K1176	NA
NLS3-EGFP	CCAGAGAAGGCCAAGAAAGCG	P1230-A1236	NA
muNLS1-EGFP (676-678)	ATAATGGAGAGCATCAAAAAGAAAAGAGCCTTGAGAAGA	R676-R688	R676I, R677M, K678E
muNLS1-EGFP (681-682)	AGAAGGAAGAGCATCGAAATAAAAAGAGCCTTGAGAAGA	R676-R688	K681E, K682I
muNLS1-EGFP (681-684)	AGAAGGAAGAGCATCGAAATAATGGGAGCCTTGAGAAGA	R676-R688	K681E, K682I, K683M, R684G
muNLS1-EGFP (687-688)	AGAAGGAAGAGCATCAAAAAGAAAAGAGCCTTGGGAATA	R676-R688	R687G, R6881

2 d after transfection cells were mock treated or treated with 100 ng/ml of tetradecanoylphorbol-13-acetate (Sigma-Aldrich) for 30 min at 37°C. Cells were collected using a rubber policeman, washed twice with ice-cold PBS, and disrupted with 30 strokes of a dounce homogenizer (pestle B) in buffer HA (10 mM Tris, pH 7.4, 150 mM NaCl, 5 mM EDTA, 1 mM PMSF, 1 mM Na_3VO_4, 1 mM NaF, complete protease inhibitor cocktail [Roche], phosphatase inhibitor cocktail II [Sigma-Aldrich]). Cell lysates were centrifuged at 1,500 *g* for 10 min to remove nuclei and intact cells. The lysates were incubated at 37°C for 30 min to augment release of 4ICD into the soluble fraction and centrifuged at 200,000 *g* for 30 min at 4°C to separate membrane and cytosolic fractions. The membrane pellets were resuspended in buffer HA containing 0.5% NP-40 (Roche). Cytosolic and membrane fractions (50 μg each) were subjected to immunoprecipitation and Western blot analysis.

Deconvolution microscopy

Cells in two-chamber slides transfected with EGFP and dsRed fusion constructs were fixed in 4% PFA for 10 min and briefly washed in PBS before coverslipping in Vectashield with DAPI (Vector Laboratories). Similarly transfected and fixed MCF-7B cells were counterstained in 500 mM DAPI (Molecular Probes) and coverslipped with Prolong Antifade Media (Molecular Probes). The slides were analyzed on a DMRXA automated upright epifluorescent microscope (Leica) equipped with a 63X (NA = 1.4) oil-immersion objective; a Sensicam QE CCD digital camera (Cooke Corporation); and filter sets optimized for EGFP (exciter HQ480/20, dichroic Q495LP, and emitter HQ510/20m), RFP (exciter 545/30×, dichroic Q570DLP, and emitter HQ620/60m), and DAPI (exciter 360/40×, dichroic 400DCLP, and emitter GG420LP). Z-axis plane capture, deconvolution, and analysis were performed with Slidebook Deconvolution Software (Intelligent Imaging Innovations).

Analysis involved the creation of an objective, digital binary overlay (mask) over arbitrary areas within regions of interest from both green and red fluorescence channels of all 3D stacks of captured planes (total of 15 per cell at 0.2 μm each) from cells demonstrating EGFP-labeled ERBB4 and RFP-labeled STAT5A. Slidebook-driven above-threshold masks were applied to 10 cells per group, fluorescence channel, and cell region to isolate both EGFP and RFP expression and discriminate or compare both EGFP and RFP cytoplasmic and nuclear expression. Analysis also entailed a pixel correlation algorithm as a measure of colocalization (or lack thereof) between the EGFP and RFP positive areas within each image (or plane) by thresholding and channel segmentation through masks. This statistical measurement determines the degree in which two voxels in a 3D stack of images correspond to one another and/or establish a spatial localization trend. If the voxels in both green and red channels arrange in an overlapping manner or colocalize entirely, then they have a correlation measurement of 1.0, and are said to be completely correlated. If the two sets of voxels correspond to each other in the exactly opposite manner, then they have a correlation measurement of −1.0, and are said to be negatively correlated. Masks were created based on pixels above threshold for each stack on a per channel and location basis. Thus, a mask was created for nuclear localization by using the DAPI channel as a template for the nucleus. A second mask was created based on green voxels in the intracellular region (including background voxels) to mask the entire cellular volume. Subsequently, the nuclear mask was subtracted from the intracellular mask to selectively create a template for intracellular expression with exclusion of nuclear volume. Both EGFP and RFP channels could then be specifically masked through those templates to identify and localize their respective voxels to those areas. A digital, background subtraction then followed. Thresholding and channel segmentation through masks were also used to measure the mean ERBB4-EGFP intensity in individual cells throughout their 3D multi-plane digital rendering. The seventh plane from a z-axis stack deconvolved through a "Nearest Neighbors" algorithm was extracted for representative and qualitative purposes only.

Extraction of nuclear and membrane/cytosolic proteins

Nuclear and membrane/cytosolic proteins were extracted using a modified version of celLytic/nuClear (Sigma-Aldrich). In brief, at 2 d after transfection MCF-7B cells in 100-mm tissue culture dishes were mock stimulated or treated with 50 ng/ml of HRG in PBS for 30 min at RT. Treated cells were washed with ice-cold PBS, collected into 5 ml of PBS by scraping, and pelleted by centrifugation. The resultant pellets were resuspended into 150 μl of hypotonic lysis buffer (10 mM Hepes, pH 7.9, 1.5 mM $MgCl_2$ 10 mM KCl) containing complete protease inhibitor cocktail (Roche) and phosphatase inhibitor cocktail II (Sigma-Aldrich) and incubated on ice for 15 min. 6 μl of 10% IGEPAL CA630 was added, samples were vortexed for 10 s and then centrifuged for 30 s at 4°C in an Eppendorf centrifuge. The resultant supernatant representing the membrane/cytosolic fraction was recovered and stored at −70°C until use. The nuclear pellet was washed in 1.0 ml of cold PBS, resuspended into 70 μl of extraction buffer (20 mM Hepes, pH 7.9, 1.5 mM $MgCl_2$, 420 mM $NaCl_2$, 0.2 mM EDTA, 25% glycerol) containing protease and phosphatase inhibitors, and vortexed for 30 min at 4°C. Samples were centrifuged for 15 min at 4°C in an eppendorf centrifuge. The resultant nuclear extracts were quick frozen in liquid nitrogen, and stored at −70°C until use. For Western blot analysis 25 μl of each membrane/cytosolic and nuclear extract was separated on a 7.5% polyacrylamide gel and transferred to Hybond ECL membrane.

Immunofluorescence

NIH 3T3 derived cell lines modified to express ERBB4-Flag (NIH-H4) or ERBB4muNLS-Flag (NIH-H4muNLS) were plated on glass coverslips coated with Cell-Tak (BD Biosciences). The cells were allowed to adhere for 18 h. The cell lines were mock stimulated or stimulated with 50 ng/ml of HRG for 30 min at RT, fixed with 4% formaldehyde in PBS for 15 min at RT, and the coverslips were washed three times for 5 min each wash in ice-cold PBS. Cells were permeabilized by incubating in blocking buffer (5% goat serum and 0.2% Tween 20 in PBS) for 30 min. Coverslips were incubated with 1:1,000 dilution of anti-Flag M2 (Sigma-Aldrich) in blocking buffer for 90 min. Coverslips were washed three times as above, and incubated for 30 min with a 1:1,000 dilution of Alexafluor 488–conjugated goat anti–mouse IgG (Molecular Probes) in blocking buffer. After three washes, cells were counterstained in 10 mM Hoechst solution in PBS for 15 min. Coverslips were washed twice and mounted with Prolong gold (Molecular Probes).

Luciferase assay

Transfections were performed on MCF-7B cells as described above with combinations of ERBB4 and STAT5A expression plasmids and a β-casein promoter luciferase reporter plasmid (provided by L. Hennighausen, National Institutes of Health, Bethesda, MD). Cell lysates were prepared at 2 d after transfection in 500 μl of cell culture lysis reagent (Promega) and luciferase assay was performed on 30 μl of lysate using the luciferase assay system (Promega) in a Berthold AutoLumat Plus luminometer. Each sample was performed in duplicate and the data represent the mean of at least three independent experiments. Statistically significant differences between datasets were determined using the paired *t* test.

ChIP assay

Association of ERBB4 and STAT5A at the endogenous β-casein promoter was determined using a modification of the ChIP assay described elsewhere (Barre et al., 2003). T47D breast cancer cells which express detectable levels of both ERBB4 and STAT5A were grown to 80% confluency on two 150 mm tissue culture dishes for each experimental treatment ($\sim 5 \times 10^7$ cells). The cells were serum starved overnight by changing the growth media to media containing 0.2% FBS and then mock stimulated with PBS or stimulated for 30 min with 5 μg/ml of ovine Prl (Sigma-Aldrich) or 50 ng/ml of HRG. Cells were washed with PBS then cross-linked with 1% PFA in PBS for 10 min at RT. The fixed cells were removed with a cell scraper, washed twice in PBS, resuspended into 2.0 ml of lysis buffer (50 mM Tris, pH 8.0, 10 mM EDTA, 1% SDS, 1 mM PMSF, complete protease inhibitor [Roche], phosphatase inhibitor cocktail II [Sigma-Aldrich]), and sonicated three times for 15 s using a small probe in a Fisher Sonic Dismembrator model 300 set at 35%. Cellular debris was removed by centrifugation at 12,000 rpm for 10 min at 4°C and the lysate was brought up to a final volume of 5.0 ml with dilution buffer (20 mM Tris, pH 8.0, 2 mM EDTA, 150 mM NaCl, 1% NP-40 [Roche], 1 mM PMSF, complete protease inhibitor, phosphatase inhibitor cocktail II). The lysate was precleared by incubating for 2 h at 4°C with 100 μl of protein A Sepharose (Amersham Biosciences), 10 μg/ml of salmon sperm DNA, and 10 μg of rabbit IgG (Santa Cruz Biotechnology, Inc.). Input chromatin was prepared from 500 μl of precleared lysate and processed along with the immunoprecipitations at the cross-link reversal step. Immunoprecipitations were performed overnight at 4°C on 1.0 ml of precleared lysate with 2 μg of rabbit anti-ERBB4 C-18 (Santa Cruz Biotechnology, Inc.) or rabbit anti-STAT5A L-20 (Santa Cruz Biotechnology, Inc.). Immune complexes were removed by adding 40 μl of a 50% protein A Sepharose slurry for 1 h at 4°C. The immunoprecipitates were washed twice for 10 min each with TSE I (20 mM Tris, pH 8.0, 2 mM EDTA, 150 mM NaCl, 1% NP-40, 0.1% SDS, 1 mM PMSF, complete protease inhibitor), TSE II (20 mM Tris, pH 8.0, 2 mM EDTA, 500 mM NaCl, 1% NP-40, 0.1% SDS, 1 mM PMSF, complete protease inhibitor), buffer III (10 mM Tris, pH 8.0, 1 mM EDTA, 250 mM LiCl, 1% NP-40, 1% deoxycholate, 1 mM PMSF, complete protease inhibitor), and finally three washes with TE buffer. Bound complexes were eluted

three times for 10 min with 200 μl of 1% SDS, 100 mM $NaHCO_3$ and formalin cross-links were reversed by incubating the eluates at 65°C overnight. The samples were digested by adding 80 μg of proteinase K for 1 h at 55°C, extracted once with phenol/chloroform/isoamyl alcohol, and nucleic acids were precipitated with 10 μg of t-RNA (Sigma-Aldrich) carrier using standard techniques. The dried nucleic acid pellet was resuspended into 50 μl of ddH_2O and 5 μl was used for each 35 cycle PCR. The input controls were used at a dilution of 1/100. The PCR primers 5′-GATGAGCATTACAAGGATATG and 5′-TAAGCTGAGTATAGACCTAC were designed to amplify a region of the β-casein promoter containing three potential distal STAT5A binding sites (−4719 to −4276; Winklehner-Jennewein et al., 1998) and the PCR primers 5′-ACTGTCCTCCAGTCATTGTCT and 5′-TGGTCCATCAGCTTCTGTGAC were designed to amplify a region of the β-casein promoter containing a proximal STAT5A binding site (−249 to −1; Winklehner-Jennewein et al., 1998). As a negative control the PCR primers 5′-GACAGATCTGAGTCCAACTGG and 5′-GGAATCTGGGTGGCTTGTATAGG were designed to amplify a region of the β-casein promoter lacking STAT5A binding sites (−923 to −590; Winklehner-Jennewein et al., 1998).

Online supplemental material

Fig. S1 shows that the ERBB4-EGFP and dsRed-STAT5A fusion proteins retain normal signaling activities. Fig. S2 demonstrates that ERBB4muNLS, harboring mutational inactivation of ERBB4 NLS1 (K681E, K682I, K683M, R684G), undergoes normal growth factor-stimulated activation and proteolytic processing to release the 4ICD. Fig. S3 shows that ERBB4muNLS stably expressed in NIH 3T3 cells fails to translocate to the nucleus after HRG stimulation. Online supplemental material is available at http://www.jcb.org/cgi/content/full/jcb.200403155/DC1.

This work is dedicated to the memory of Marco Mannino, a loving father and husband, inspirational teacher and friend, and spirited jazz musician; taken from us by multiple myeloma.

We thank Cesar Fermin of the Centralized Tulane Imaging Center for advice on deconvolution microscopy. We thank Diane Clark for excellent lab management, Amy Notwick for editing this manuscript, Keadren Green and Debbie Lauff for administrative assistance, and members of the Jones lab for thoughtful suggestions. We are grateful to Carolyn Sartor for providing ERBB4KD and Lothar Hennighausen for providing the β-casein luciferase construct.

This work was supported by National Institutes of Health/National Cancer Institute grants RO1CA095783 (to F.E. Jones) and RO1CA096717 (to F.E. Jones), US Army Medical Research and Material Command grant DAMD17-03-1-0395 (to G.A. Vidal), and funds generously provided by the National Cancer Coalition and the Tulane Cancer Center.

Submitted: 29 March 2004
Accepted: 23 September 2004

Note added in proof. While this manuscript was in press, evidence of ERBB2 nuclear translocation and binding to the COX-2 promoter was published (Wang, S.C., H.C. Lien, W. Xia, I.F. Chen, H.W. Lo, Z. Wang, M. Ali-Seyed, D.F. Lee, G. Bartholomeusz, F. Ou-Yang, D.K. Giri, and M.C. Hung. 2004. Binding at and transactivation o fthe COX-2 promoter by nuclear tyrosine kinase receptor ErbB-2. *Cancer Cell.* 6:251–261.

References

Barre, B., S. Avril, and O. Coqueret. 2003. Opposite regulation of myc and p21waf1 transcription by STAT3 proteins. *J. Biol. Chem.* 278:2990–2996.

Burow, M.E., C.B. Weldon, Y. Tang, J.A. McLachlan, and B.S. Beckman. 2001. Oestrogen-mediated suppression of tumour necrosis factor alpha-induced apoptosis in MCF-7 cells: subversion of Bcl-2 by anti-oestrogens. *J. Steroid Biochem. Mol. Biol.* 78:409–418.

Elenius, K., G. Corfas, S. Paul, C.J. Choi, C. Rio, G.D. Plowman, and M. Klagsbrun. 1997. A novel juxtamembrane domain isoform of HER4/ErbB4: isoform-specific tissue distribution and differential processing in response to phorbol ester. *J. Biol. Chem.* 272:26761–26768.

Gassmann, M., F. Casagranda, D. Orioli, H. Simon, C. Lai, R. Klein, and G. Lemke. 1995. Aberrant neural and cardiac development in mice lacking the ErbB4 neuregulin receptor. *Nature.* 378:390–394.

Herrington, J., L. Rui, G. Luo, L.-Y. Yu-Lee, and C. Carter-Su. 1999. A functional DNA binding domain is required for growth hormone-induced nuclear accumulation of Stat5B. *J. Biol. Chem.* 274:5138–5145.

Jones, F.E., T. Welte, X.-Y. Fu, and D.F. Stern. 1999. ErbB4 signaling in the mammary gland is required for lobuloalveolar development and Stat5 activation during lactation. *J. Cell Biol.* 147:77–87.

Jones, F.E., J.P. Golding, and M. Gassmann. 2003. ErbB4 signaling during breast and neural development: novel genetic models reveal unique ErbB4 activities. *Cell Cycle.* 2:555–559.

Komuro, A., M. Nagai, N.E. Navin, and M. Sudol. 2003. WW domain-containing protein YAP associates with ErbB-4 and acts as a co-transcriptional activator for the carboxyl-terminal fragment of ErbB-4 that translocates to the nucleus. *J. Biol. Chem.* 278:33334–33341.

Kudo, N., N. Matsumori, H. Taoka, D. Fujiwara, E.P. Schreiner, B. Wolff, M. Yoshida, and S. Horinouchi. 1999. Leptomycin B inactivates CRM1/exportin 1 by covalent modification at a cysteine residue in the central conserved region. *Proc. Natl. Acad. Sci. USA.* 96:9112–9117.

Lamond, A.I., and D.L. Spector. 2003. Nuclear speckles: a model for nuclear organelles. *Nat. Rev. Mol. Cell Biol.* 4:605–612.

Lee, H.J., K.M. Jung, Y.Z. Huang, L.B. Bennett, J.S. Lee, L. Mei, and T.W. Kim. 2002. Presenilin-dependent γ-secretase-like intramembrane cleavage of ErbB4. *J. Biol. Chem.* 277:6318–6323.

Lin, S.Y., K. Makino, W. Xia, A. Matin, Y. Wen, K.Y. Kwong, L. Bourguignon, and M.C. Hung. 2001. Nuclear localization of EGF receptor and its potential new role as a transcription factor. *Nat. Cell Biol.* 3:802–808.

Long, W., K.-U. Wagner, K.C.K. Lloyd, N. Binart, J.M. Shillingford, L. Hennighausen, and F.E. Jones. 2003. Impaired differentiation and lactational failure in ErbB4-deficient mammary glands identify ERBB4 as an obligate mediator of Stat5. *Development.* 130:5257–5268.

Melen, K., L. Kinnunen, and I. Julkunen. 2001. Arginine/lysine-rich structural element is involved in interferon-induced nuclear import of STATs. *J. Biol. Chem.* 276:16447–16455.

Meyer, T., A. Begitt, I. Lodige, M. van Rossum, and U. Vinkemeier. 2002. Constitutive and IFN-gamma-induced nuclear import of STAT1 proceed through independent pathways. *EMBO J.* 21:344–354.

Meyer, T., A. Marg, P. Lemke, B. Wiesner, and U. Vinkemeier. 2003. DNA binding controls inactivation and nuclear accumulation of the transcription factor Stat1. *Genes Dev.* 17:1992–2005.

Ni, C.-Y., M.P. Murphy, T.E. Golde, and G. Carpenter. 2001. γ-Secretase cleavage and nuclear localization of ErbB-4 receptor tyrosine kinase. *Science.* 294:2179–2181.

Ni, C.Y., H. Yuan, and G. Carpenter. 2003. Role of the ErbB-4 carboxyl terminus in γ-secretase cleavage. *J. Biol. Chem.* 278:4561–4565.

Offterdinger, M., C. Schofer, K. Weipoltshammer, and T.W. Grunt. 2002. c-erbB-3: a nuclear protein in mammary epithelial cells. *J. Cell Biol.* 157:929–939.

Plowman, G.D., G.S. Whitney, M.G. Neubauer, J.M. Green, V.L. McDonald, G.J. Todaro, and M. Shoyab. 1990. Molecular cloning and expression of an additional epidermal growth factor receptor-related gene. *Proc. Natl. Acad. Sci. USA.* 87:4905–4909.

Plowman, G.D., J.-M. Culouscou, G.S. Whitney, J.M. Green, G.W. Carlton, L. Foy, M.G. Neubauer, and M. Shoyab. 1993. Ligand-specific activation of HER4/p180^{erbB4}, a fourth member of the epidermal growth factor receptor family. *Proc. Natl. Acad. Sci. USA.* 90:1746–1750.

Riese, D.J., II, T.M. van Raaij, G.D. Plowman, G.C. Andrews, and D.F. Stern. 1995. Cellular response to neuregulins is governed by complex interactions of the erbB receptor family. *Mol. Cell. Biol.* 15:5770–5776.

Rio, C., J.D. Buxbaum, J.J. Peschon, and G. Corfas. 2000. Tumor necrosis factor-alpha-converting enzyme is required for cleavage of erbB4/HER4. *J. Biol. Chem.* 275:10379–10387.

Sartor, C.I., H. Zhou, E. Kozlowska, K. Guttridge, E. Kawata, L. Caskey, J. Harrelson, N. Hynes, S. Ethier, B. Calvo, and H.S. Earp III. 2001. HER4 mediates ligand-dependent antiproliferative and differentiation responses in human breast cancer cells. *Mol. Cell. Biol.* 21:4265–4275.

Schroeter, E.H., J.A. Kisslinger, and R. Kopan. 1998. Notch-1 signalling requires ligand-induced proteolytic release of intracellular domain. *Nature.* 393:382–386.

Srinivasan, R., C.E. Gillett, D.M. Barnes, and W.J. Gullick. 2000. Nuclear expression of the c-erbB-4/HER4 growth factor receptor in invasive breast cancers. *Cancer Res.* 60:1483–1487.

Tidcombe, H., A. Jackson-Fisher, K. Mathers, D.F. Stern, M. Gassmann, and J.P. Golding. 2003. Neural and mammary gland defects in ErbB4 knockout mice genetically rescued from embryonic lethality. *Proc. Natl. Acad. Sci. USA.* 100:8281–8286.

Winklehner-Jennewein, P., S. Geymayer, J. Lechner, T. Welte, L. Hansson, S. Geley, and W. Doppler. 1998. A distal enhancer region in the human beta-casein gene mediates the response to prolactin and glucocorticoid hormones. *Gene.* 217:127–139.